Biochemical and Biophysical Research Communications 421 (2012) 757–762

Contents lists available at SciVerse ScienceDirect

Biochemical and Biophysical Research Communications

journal homepage: www.elsevier.com/locate/ybbrc

Structural insights into the metabolism of 2-chlorodibenzofuran by an evolved biphenyl dioxygenase

Pravindra Kumar [b,c], Mahmood Mohammadi [a,1], Sonali Dhindwal [c], Thi Thanh My Pham [a], Jeffrey T. Bolin [b], Michel Sylvestre [a,*]

[a] Institut National de la Recherche Scientifique (INRS-Institut Armand-Frappier), Laval, QC, Canada H7V 1B7
[b] Department of Biological Sciences and Center for Cancer Research, Purdue University, West Lafayette, IN 47907, USA
[c] Department of Biotechnology, Indian Institute of Technology, Roorkee 247667, India

ARTICLE INFO

Article history:
Received 30 March 2012
Available online 22 April 2012

Keywords:
Rieske-type oxygenase
Directed evolution
Burkholderia xenovorans LB400
Chlorodibenzofurans
Biocatalysis
Enzyme engineering

ABSTRACT

The biphenyl dioxygenase of *Burkholderia xenovorans* LB400 ($BphAE_{LB400}$) is a Rieske-type oxygenase that catalyzes the stereospecific oxygenation of many heterocyclic aromatics including dibenzofuran. In a previous work, we evolved $BphAE_{LB400}$ and obtained $BphAE_{RR41}$. This variant metabolizes dibenzofuran and 2-chlorodibenzofuran more efficiently than $BphAE_{LB400}$. However, the regiospecificity of $BphAE_{RR41}$ toward these substrates differs. Dibenzofuran is metabolized principally through a lateral dioxygenation whereas 2-chlorodibenzofuran is metabolized principally through an angular dioxygenation. In order to explain this difference, we examined the crystal structures of both substrate-bound forms of $BphAE_{RR41}$ obtained under anaerobic conditions. This structure analysis, in combination with biochemical data for a Ser283Gly mutant provided evidences that the substrate is compelled to move after oxygen-binding in $BphAE_{RR41}$:dibenzofuran. In $BphAE_{RR41}$:2-chlorodibenzofuran, the chlorine atom is close to the side chain of Ser283. This contact is missing in the $BphAE_{RR41}$:dibenzofuran, and strong enough in the $BphAE_{RR41}$:2-chlorodibenzofuran to help prevent substrate movement during the catalytic reaction.

1. Introduction

Prototrophic soil bacteria are major contributors to the process of mineralization of organic matter because they can use a large array of organic compounds as a source of carbon and energy. The sequential enzymatic reactions involved in this process are organized into pathways. The ability of enzymes of these pathways to undergo a relaxation of their specificities toward a range of structurally distinct substrates without the loss of function is of critical importance to expand metabolic versatility. The bacterial biphenyl catabolic pathway represents an example of an emerging pathway for the degradation of several man-made persistent pollutants such as polychlorinated biphenyls (PCBs) [1] and polychlorinated dibenzofurans [2].

The biphenyl dioxygenase (BPDO) catalyzes the first step of the biphenyl/PCB catabolic pathway. This Rieske-type dioxygenase (RO) metabolizes many biphenyl analogs including ethyl-, vinyl-, carboxyl-, halogenated- or nitro-substituted benzenes or diphenyls [3–9]. It also oxygenates bicyclic- or tricyclic-fused heterocyclic aromatics such as dibenzofuran and flavonoids [2,7]. The enzyme catalyzes a stereospecific dioxygenation reaction to generate a *cis*-dihydrodiol metabolite (Fig. 1). In the context of the green chemistry concept, more selective and environment friendly approaches to manufacture biologically specific fine chemicals will be required in future. This includes the use of biocatalysts such as ROs [3,10]. Therefore, understanding how BPDO catalytic pocket interacts with its substrates to bind them and orient their reactive carbons toward the protein reactive atoms will help design novel biocatalysts useful in biotechnological processes for the destruction of persistent pollutants or biocatalytic processes for green production of chemicals.

BPDO comprises three components [11–13]. The catalytic component, which is a RO protein (BphAE) is a hetero hexamer made up of three α (BphA) and three β subunits (BphE). The other two components are the ferredoxin (BphF) and the ferredoxin reductase (BphG) which are involved in the electron transfer from NADH to BphAE [12].

Burkholderia xenovorans LB400 BphAE ($BphAE_{LB400}$) has been thoroughly investigated because this organism is considered as one of the best PCB degrader of natural occurrence [14]. Using a semi-rational directed-evolution approach, we evolved $BphAE_{LB400}$ and obtained $BphAE_{p4}$ [15] and $BphAE_{RR41}$ [2]. These two variants

Abbreviation: BPDO, biphenyl dioxygenase; CARDO, carbazole dioxygenase; CARDO-O, carbazole dioxygenase large subunit; PCB, polychlorinated biphenyl; RO, Rieske-type oxygenase.

* Corresponding author. Fax: +1 450 686 5501.
E-mail address: Michel.Sylvestre@iaf.inrs.ca (M. Sylvestre).
[1] Present address: Département de génie informatique et génie logiciel, École Polytechnique de Montréal, C.P. 6079, succ. Centre-ville, Montréal, QC, Canada H3C 3A7.

0006-291X/$ - see front matter © 2012 Elsevier Inc. All rights reserved.
http://dx.doi.org/10.1016/j.bbrc.2012.04.078

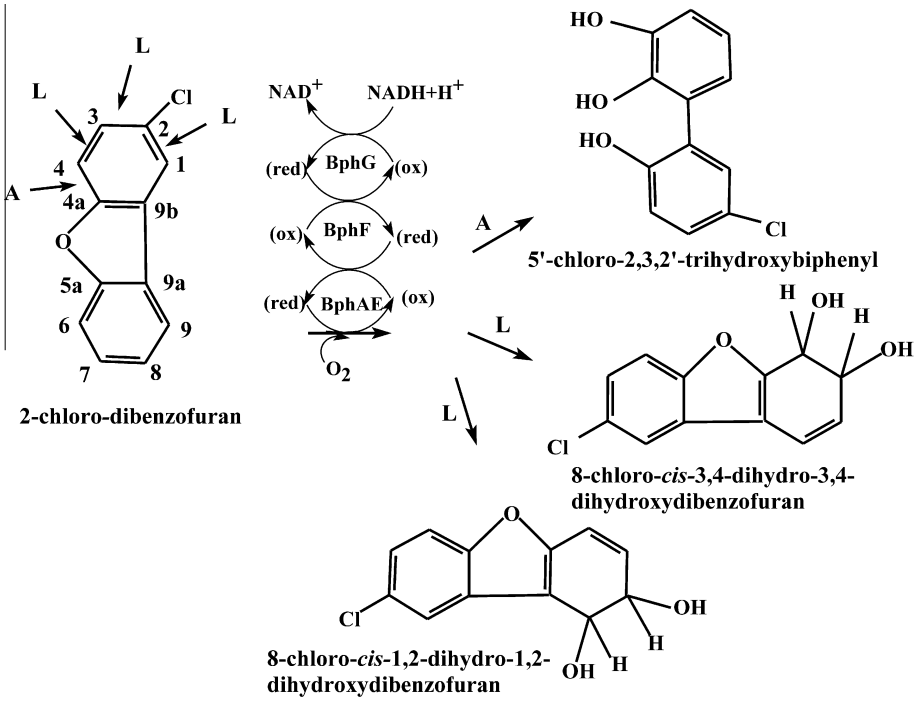

Fig. 1. The biphenyl dioxygenase reaction with 2-chlorodibezofuran as substrate. The figure shows the various metabolites that can be produced from 2-chlorodibenzofuran depending on the mode of attack (L, lateral or A, angular).

metabolize a much broader range of substrates than the parent enzyme [2,15,16]. Structural analyses showed that Thr335Ala substitution, common to both variants relieved intramolecular constraints on the Val320Gly321Gln322 segment lining the catalytic pocket allowing for a significant movement of this segment during the substrate binding, thus increasing the space available to accommodate larger substrates [14]. In addition, we found that the combined Asn338Gln Leu409Phe substitutions of $BphAE_{RR41}$ altered a substrate-induced mechanism required to retune the alignment of protein atoms involved in the chemical steps of the reaction [14]. This mechanism speeds up the electron transport process during the catalytic reaction. As a result, the enzyme was able to catalyze the oxygenation of dibenzofuran and chlorodibenzofurans [2,14] as well as of PCBs [16] more efficiently than the parent enzyme.

In a previous report, we found that unlike the carbazole dioxygenase (CARDO) [17] $BphAE_{LB400}$ and $BphAE_{RR41}$ metabolized dibenzofuran principally through a lateral dioxygenation to generate *cis*-1,2-dihydro-1,2-dihydroxydibenzofuran as a major metabolite [2]. However, structural analysis of the dibenzofuran-bound $BphAE_{RR41}$ showed the substrate is in the orientation that would enable a 4, 4a angular attack [18]. This suggested a displacement of the substrate during one of the steps of the catalytic process [18].

An interesting feature of $BphAE_{RR41}$ was its ability to metabolize chlorinated dibenzofurans [2]. Unlike dibenzofuran, 2-chlorodibenzofuran was metabolized to generate 5′-chloro-2,3,2′-trihydroxybiphenyl as the major metabolite [2]. Thus, the dioxygenation reaction occurred principally onto the angular carbons 5a and 6 corresponding to carbon 4, 4a of the non-chlorinated ring (see Fig. 1). In order to explain how the chlorine atom may contribute to the regiospecificity of the enzyme, in this work, we report the crystal structure of the 2-chlorodibenzofuran-bound $BphAE_{RR41}$ and we compare its structure to the dibenzofuran-bound enzyme. We also examine the regiospecificity of a Ser283Gly mutant of $BphAE_{RR41}$ towards 2-chlorodibenzofuran.

2. Materials and methods

2.1. Purification, crystallization and structural analysis

His-tagged $BphAE_{RR41}$ was produced in *Escherichia coli* C41(DE3) from pET14b. It was purified by affinity chromatography and then the His-tag was removed according to previously described protocols [18]. The procedures to prepare crystals of the 2-chlorodibenzofuran-bound form of $BphAE_{RR41}$ under anaerobic conditions were similar to those described for the dibenzofuran-bound form of $BphAE_{RR41}$ [19]. Briefly, $BphAE_{RR41}$ crystals grew in monoclinic space group $P2_1$ with six $\alpha\beta$ dimers (i.e., two $\alpha_3\beta_3$ hexamers) in the asymmetric unit at 21 °C when the reservoir solution (1000 μl) contained 20–25% (w/v) PEG 8000, 50 mM PIPES pH 6.5, 100 mM ammonium acetate and 0.2% (w/v) agarose. Diffraction data were collected at 100 K using synchrotron radiation (SER-CAT beamline 22-ID at the Advanced Photon Source, Chicago, USA). The diffraction patterns were indexed, integrated and scaled using the *HKL2000* suite [20].

The crystal structure of $BphAE_{RR41}$:2-chlorodibenzofuran was solved by the molecular replacement method using MOLREP [21] from the *CCP4* v.6.2.0 software suite [22]. The $BphAE_{RR41}$:2-chlorodibenzofuran model was refined using the program CNS [23] and REFMAC5.2 [24]. Non-crystallographic symmetry restraints were used initially. At later stages of refinement, these restraints were completely released. This structure was analysed using approaches similar to those used for $BphAE_{RR41}$ [14]. The complex structure was compared with the crystal structures of $BphAE_{LB400}$ (RCSB Protein Data accession code: 2XR8) and its biphenyl-bound form (2XRX) and those of $BphAE_{RR41}$ (RCSB Protein Data accession code: 2YFI) and its dibenzofuran-bound form (2YFJ). It was also compared to the carbazole-bound form of CARDO large subunit (CARDO-O) (RCSB Protein Data accession code: 2DE7) [25]. The CASTp program [26] which is available online (http://sts.bioengr.uic.edu/castp/index.php) was used to calculate the catalytic

cavity volume using a probe radius of 1.4 Å. Figures were prepared using the program PyMOL [27].

2.2. Enzyme assays and metabolite analysis

Site-directed mutagenesis of *bphA* variant RR41 was performed to substitute Ser283 to Gly using a two-step mutagenesis protocol as described previously [2]. Reconstituted His-tagged BPDO preparations were used in these experiments. His-tagged purified enzyme components were produced in recombinant *E. coli* strains and purified according to the published protocols [18]. The enzyme assays were performed at 37 °C as described previously in a volume of 200 µl in 50 mM morpholinethanesulfonic (MES) buffer pH 6.0, containing 100 nmol of substrate [13]. The metabolites were extracted at pH 6.0 with ethyl acetate and treated with *N,O-bis*(trimethylsilyl)trifluoroacetamide (BSTFA) (Supelco, Sigma – Aldrich) as described previously for gas-chromatography mass spectrometry (GC–MS) analysis [2].

2.3. PDB accession codes

The coordinates and the structure factors of 2-chlorodibenzofuran:BphAE$_{RR41}$ complex have been deposited with the RCSB Protein Data Bank (http://deposit.rcsb.org/) using Autodep (http://www.ebi.ac.uk/pdbe-xdep/autodep/) under the accession code 2YFL.

3. Results and discussion

The overall crystal structure of the 2-chlorodibenzofuran-bound form of BphAE$_{RR41}$ is very similar to its dibenzofuran-bound form [18]. They both contain triplets of $\alpha\beta$ dimers that associate to generate two (ABCDEF and GHIJKL) hexamers in an asymmetric unit. The crystals of 2-chlorodibenzofuran-complex were obtained in the monoclinic space group $P2_1$ with unit cell parameters of $a = 86.9$, $b = 277.8$, $c = 92.9$ Å and $\alpha = 90.0$, $\beta = 117.6$ and $\gamma = 90.0°$ and they diffracted to a resolution of 2.6 Å. The final refined model contains residues Asn18 to Phe143 plus Phe153 to Pro459 of the α subunit and residues Phe9 to Phe188 of the β subunit. Crystallographic data and statistics for the refined structure are reported in Table 1. Superposition of all the C^{α} atoms of chains AB and chains CD to chains KL gives rmsd values of 0.3–0.4 Å^2. The most disordered residues and protein segments were the same as observed for the native and dibenzofuran-bound forms of BphAE$_{RR41}$ [18], including the segments comprising residues Ile-247 to Lys-263 and Glu-280 toVal-287 of the α subunit and 9–17 and 158–164 of the β subunit. The bound 2-chlorodibenzofuran could be identified clearly in the difference Fourier maps in the active sites of dimers AB and CD only. The electron density map for 2-chlorodibenzofuran-bound forms of BphAE$_{RR41}$ along with the catalytic center residues for both the dimers are shown in Fig. 2.

However, in dimer CD, the substrate was not in a productive orientation since no pair of neighboring carbon atoms are superposed with the reactive atoms of dibenzofuran in BphAE$_{RR41}$:dibenzofuran (Fig. 3) or of biphenyl in BphAE$_{LB400}$: biphenyl (not shown). In contrast, in the case of BphAE$_{RR41}$:dibenzofuran crystal structure, the three dimers for which the substrate showed sufficient density to be identified in the Fourier maps, were all in a productive orientation [18]. The fact that 2-chlorodibenzofuran may bind the enzyme in a non-productive orientation explains why the specificity (kcat/km value) of BphAE$_{RR41}$ reported earlier [2] for 2-chlorodibenzofuran (9×10^3 M^{-1} s^{-1}) was significantly lower than for dibenzofuran (5×10^4 M^{-1} s^{-1}).

When dimers AB of BphAE$_{RR41}$:dibenzofuran and of BphAE$_{RR41}$:2-chlorodibenzofuran are superposed, the position of the oxidized carbons, C4a and C4 of both the substrates are nearly the same (Fig. 3). Both dibenzofuran and 2-chlorodibenzofuran are in the orientation that would enable a 4, 4a angular attack. As pointed out previously, this was unexpected for dibenzofuran since biochemical data revealed that 2,3,2′-trihydroxybiphenyl resulting from the angular attack of dibenzofuran was produced in trace amounts whereas 1,2-dihydro-1,2-dihydroxydibenzofuran was by far the major metabolite. We explained this apparent discrepancy by the fact that the crystals of BphAE$_{RR41}$:dibenzofuran structure that we reported were obtained under anaerobic conditions [19], in a state prior to oxygen-binding [18]. In a manner similar to the previously reported structure of BphAE$_{RR4}$:dibenzofuran [18] (Fig. 4A), in this state, a polar contact is formed between the furan's oxygen ring of 2-chlorodibenzofuran and the water ligand on the active site's Fe^{++} (Fig. 4B).

The crystals of BphAE$_{RR41}$:2-chlorodibenzofuran were obtained using the same procedures as described previously for BphAE$_{RR41}$:dibenzofuran [19]. Based on the reaction cycle for ROs proposed by Karlsson et al. [28], when a dioxygen binds, it intercalates side-on between the iron and the substrate, displacing the water ligand. This suggests that in a state that follows oxygen-binding, the substrate is compelled to move and to change its orientation. Therefore, the fact that unlike dibenzofuran, 2-chlorodibenzofuran is metabolized principally through an angular mode of attack by BphAE$_{RR41}$ suggests that interactions between protein structures and the chlorine atom of 2-chlorodibenzofuran help prevent substrate movement during the catalytic reaction.

Superposition of dimers AB of BphAE$_{RR41}$:dibenzofuran and of BphAE$_{RR41}$:2-chlorodibenzofuran shows the corresponding carbon atoms of 2-chlorodibenzofuran and of dibenzofuran interact with the same residues of BphAE$_{RR41}$ α subunit (not shown) (Gln226,

Table 1
Crystallographic data and refinement results for BphAE$_{RR41}$:2-chlorodibenzofuran structure.

Crystallographic data	
Space group	$P2_1$
Wavelength	1.0
Resolution	100–2.6
Cell dimensions	
a (Å)	86.6
b (Å)	276.0
c (Å)	92.1
β (°)	117.5
Unique reflections	97588
Completeness (%) (Last shell)	80.1 (49.0)
R_{sym}(%)[a] (Last Shell)	14 (51.0)
I/σ (Last shell)	11.9 (2.0)
Multiplicity (Last shell)	3.1 (2.1)
Refinement	
No. of residues	3720
Water molecules	158
Resolution range (Å)	100–2.6
R_{fact} (%)	21.9
R_{free} (%)	28.1
Average *B*-factors (Å^2)	AB 52.1, 49.4
	CD 55.7, 50.4
	EF 52.5, 52.0
	GH 64.3, 56.3
	IJ 65.5, 58.0
	KL 70.0, 57.0
Waters	43.6
All atoms	29812
Bond lengths (Å)	0.01
Bond angles (°)	0.92
Ramachandran plot (%)	
Preferred	87.2
Allowed	12.6
Outliers	0.2

[a] $R_{sym} = \sum_{hkl}\sum_{i=1}^{n}|I_{hkl,i} - \bar{I}_{hkl}| / \sum_{hkl}\sum_{i=1}^{n} I_{hkl,i}$.

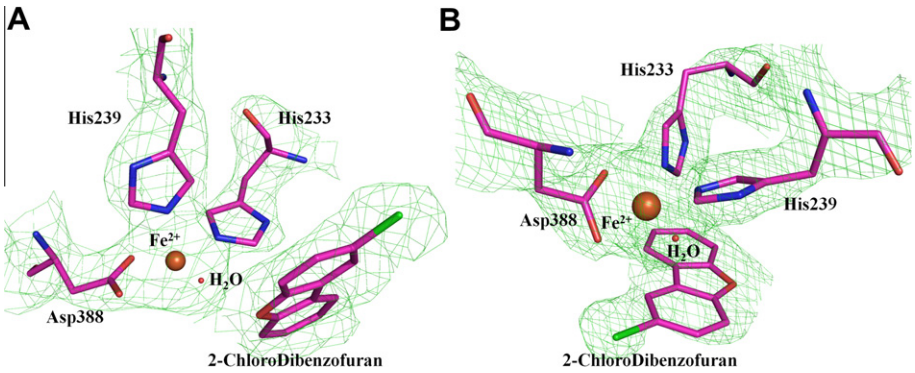

Fig. 2. The $2F_{obs}-F_{calc}$ electron density map of 2-chlorodibenzofuran-bound $BphAE_{RR41}$ contoured at 1.0 σ level. (A) Chain AB, (B) Chain CD.

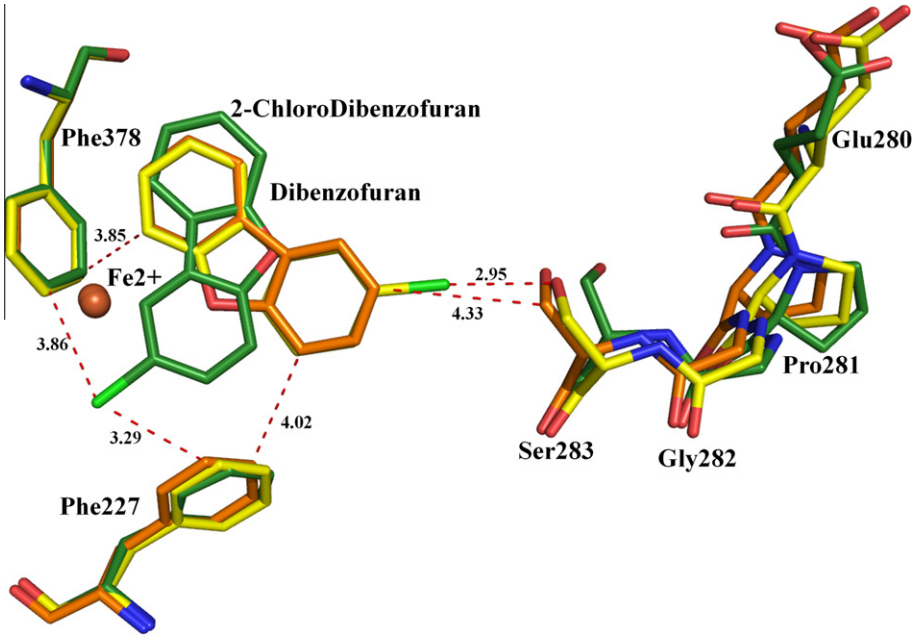

Fig. 3. Superposition of dimers AB (yellow) and CD (green) of $BphAE_{RR41}$:2-chlorodibenzofuran and of dimer AB of $BphAE_{RR41}$:dibenzofuran (orange). The figure shows 2-chlorodibenzofuran is not placed in a productive orientation in dimer CD and it also shows the protein atoms that are contacting the chlorine atom of the substrate.

Phe227, Asp230, Met231, Leu233, Ala234, His323 and Leu333 for the proximal ring and Phe384, Phe378, Val287, Ser283, Phe/Met336, Leu333, Gly321, Tyr277, His239, Ala234 and Met231 for the distal ring) and they are located at approximately the same distances. However, Ser283 side-chain is much closer to the chlorine atom of 2-chlorodibenzofuran than to C-2 of dibenzofuran (Fig. 3). Furthermore, the cavity volume of $BphAE_{RR41}$:2-chlorodibenzofuran (1103 $Å^3$) as calculated from CASTp software is in the same range as for $BphAE_{RR41}$:dibenzofuran. Therefore, neither the overall size of the cavity nor the constraints on the reactive ring of the substrates differed significantly, between $BphAE_{RR41}$:dibenzofuran and $BphAE_{RR41}$:2-chlorodibenzofuran. The only difference between the two forms of the enzyme is the proximity of Ser283 to the chlorine atom on the substrate's distal ring. Therefore, structural analysis suggests that the contact between Ser283 and the chlorine of 2-chlorodibenzofuran helps prevent substrate displacement during the catalytic reaction.

In order to show that Ser283 has an influence on substrate regiospecificity, we have prepared a Ser283Gly mutant of $BphAE_{RR41}$ and we have determined the ratio of the metabolites produced from 2-chlorodibenzofuran by a purified preparation of this enzyme. On the basis of the ratios of the area under the GC–MS peaks of 2,3-dihydro-2,3-dihydroxy-8-chlorodibenzofuran and of 5-chloro-2,3,2′-trihydroxybiphenyl, which were 0.26 ± 0.0 for $BphAE_{RR41}$ and 1.7 ± 0.8 for its Ser283Gly mutant, it is clear that the regiospecificity of the mutant is altered to favor a lateral attack (see Fig. 1 for the metabolites structures).

Unlike $BphAE_{RR41}$, CARDO-O was found to catalyze an angular oxygenation of carbazole and of dibenzofuran [17] and the structure of the carbazole-bound enzyme is known [25]. Therefore, it was interesting to compare the structure of CARDO-O with that of $BphAE_{RR41}$. On the basis of structural analysis, Nojiri et. al. [29] proposed an oxygen-binding process that involves the intercalation side-on of the dioxygen between the substrate and the mononuclear Fe^{++}, in a manner similar to other ROs. Furthermore, the electron transfer system is similar to that of other RO's [29]. Therefore, both CARDO and BPDO reactions are likely to proceed through similar catalytic mechanisms. Superposition of the substrate-bound forms of $BphAE_{RR41}$ and of CARDO-O showed the residues lining the catalytic pocket do not align well and the orientation of the substrate inside their catalytic pocket differs significantly (not shown). However, the catalytic Fe^{++} and the protein atoms that coordinate it superposes very well (not shown). On the other hand, notably as reported earlier [25] the carbazole imino group

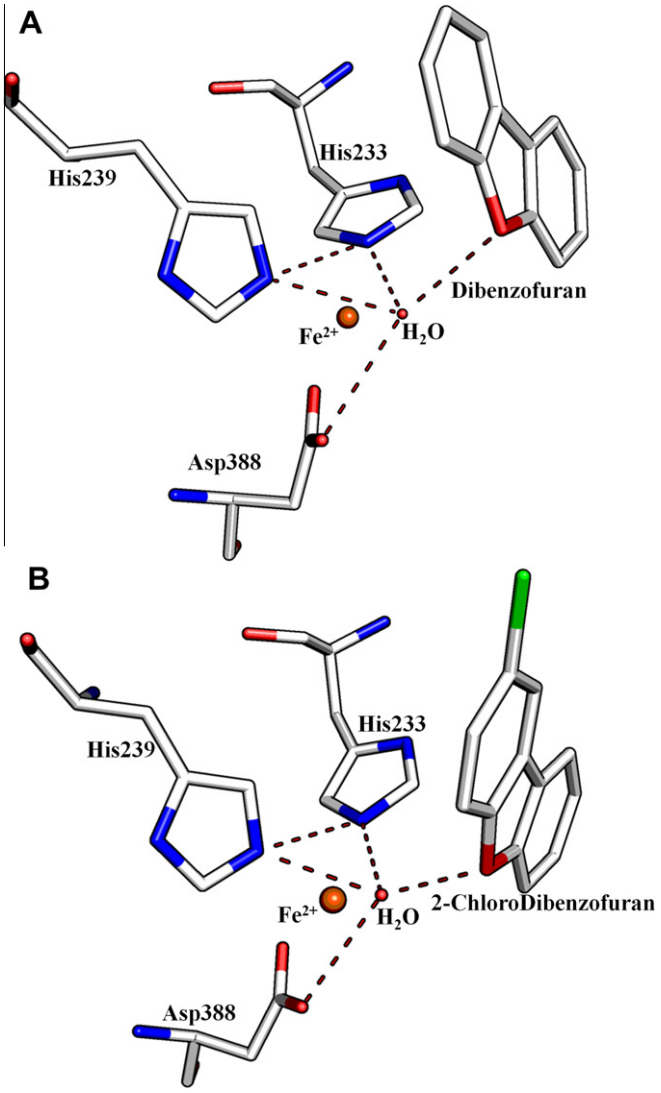

Fig. 4. Catalytic center of dimer AB of (A) $BphAE_{RR41}$:dibenzofuran and (B) $BphAE_{RR41}$:2-chlorodibenzofuran. The figure shows the water molecule contacting the furan ring's oxygen.

contacts the carbonyl of residue Gly178 which is located on a short helix of CARDO-O. The corresponding helix in $BphAE_{RR41}$ does not align well with that of CARDO-O (not shown) but it is noteworthy that it comprises residues Asp230 (corresponding to Asp180 of CARDO-O) and Gln226 that are involved in the catalytic activity of RO's proteins [30,31] and are displaced during substrate binding [18]. This comparison confirms that despite of the differences in the conformation of the catalytic pocket, these two enzymes have a similar reaction mechanism. However, in the course of evolution of CARDO-O, the polar contact between Gly178 and the imino group of carbazole has most likely been acquired as an extra structural feature that was intended to help prevent substrate movement during the catalytic reaction. Although there is no dibenzofuran-bound CARDO-O structure available, it is likely that the furan's ring oxygen contacts Gly178 of CARDO-O in a manner similar to the carbazole's imino group.

The size of the catalytic pocket of $BphAE_{LB400}$ as well as of its mutant $BphAE_{RR41}$ is in the same range as of CARDO-O and during the catalytic reaction, they exceed the size required to accommodate the substrate. We previously reported that due to the large size of the catalytic pocket, the non-reactive ring of biphenyl can access different orientations [14]. One drawback of the extra space inside the catalytic pocket, which is illustrated in the present work is that biphenyl analogs must interact strongly enough with protein atoms to prevent any movement in case of any disturbances occurring during the catalytic process. As illustrated above, in the case of CARDO, the dibenzofuran or carbazole ring is stabilized through a polar contact between protein atoms and the substrate. In the case of $BphAE_{RR41}$, the non polar contact between the chlorine atom of 2-chlorodibenzofuran and Ser283 appears sufficient to help prevent substrate movement during the binding and the catalytic processes. $BphAE_{RR41}$ does not offer the possibility of such stable contact when dibenzofuran is the substrate which may explain why $BphAE_{RR41}$ does not catalyze an angular dioxygenation of dibenzofuran.

The fact that 2-chlorodibenzofuran is not placed into a productive orientation inside the catalytic pocket of all the dimers of $BphAE_{RR41}$:2-chlorodibenzofuran shows that the 2-chlorine atom on the dibenzofuran ring exhibits a significant influence on the binding process. In dimer CD, where 2-chlorodibenzofuran does not exhibit a productive orientation, the furan ring's oxygen is far from the catalytic iron and its water ligand. However, in this case, the chlorine atom is close enough to Phe227 and Phe378 to interact strongly with these residues (Fig. 3). This shows that the chlorine atom on C-2 of dibenzofuran is not only playing a role in preventing substrate movement when it binds in the appropriate orientation for a productive reaction, but the influence this atom exerts during the binding process may be strong enough to modulate the substrate's overall orientation inside the catalytic pocket.

In recent reports, Inoue et al. [32] have observed that binding of the ferredoxin to the oxygenase component induces a movement of the oxygenase's Rieske cluster of CARDO-O, Martins et al. [33] showed that reduction of the Rieske cluster of the 2-Oxoquinoline 8-monooxygenase oxygenase component induces a conformational change that alters the active site geometry to create a pathway for dioxygen and Mohammadi et al. [18] have shown that several residues around the catalytic iron are displaced during substrate binding to BPDO. However the molecular basis of the RO's catalytic reaction and how these movements influence the chemical steps involved in the oxygenation reaction remain unclear. Furthermore, some questions are still remaining to be answered to understand the precise interaction between the substrate, the mononuclear iron and the vicinal Rieske cluster and how any movement in this complex would influence the regiospecificity as well as the ability of the enzyme to catalyze a productive reaction. Since the active site residues are displaced during the catalytic reaction and because of the large size of BPDO's catalytic pocket it is to be expected that the substrate needs to be stabilized during the catalytic reaction to prevent any movement that would affect the regiospecificity. In this context, our structural and biochemical data provide evidence that for some biphenyl analogs such as dibenzofuran, the interactions with protein atoms are too weak to prevent substrate movement. However, the presence of a chlorine substituent that strongly interacts with protein atoms appears to be sufficient to prevent substrate displacement and to significantly affect the outcome of the reaction.

Acknowledgments

This work was supported by the Natural Sciences and Engineering Research Council of Canada (NSERC) (Grant #RGPIN/39579-2007). X-ray diffraction data were collected at APS using Southeast Regional Collaborative Access Team (SER-CAT) 22-ID beamline; supporting institutions may be found at http://ser-cat.org/members.html. PK thanks the DRDO, India for providing the financial

support and also thank MCU facility at IIC, IIT Roorkee for carrying out structure determination and analysis.

References

[1] M. Sylvestre, J.P. Toussaint, Engineering microbial enzymes and plants to promote PCB degradation in soil: Current state of knowledge, in: A.I. Koukkou (Ed.), Microbial Bioremediation of Non-metals Current Research, Caister Academic Press, Norfolk, U.K., 2011, pp. 177–196.
[2] M. Mohammadi, M. Sylvestre, Resolving the profile of metabolites generated during oxidation of dibenzofuran and chlorodibenzofurans by the biphenyl catabolic pathway enzymes, Chem. Biol. 12 (2005) 835–846.
[3] D.R. Boyd, T.D.H. Bugg, Arene *cis*-dihydrodiol formation: From biology to application, Org. Biomol. Chem. 4 (2006) 181–192.
[4] H.K. Chun, Y. Ohnishi, K. Shindo, N. Misawa, K. Furukawa, S. Horinouchi, Biotransformation of flavone and flavanone by *Streptomyces lividans* cells carrying shuffled biphenyl dioxygenase genes, J. Mol. Catal. B: Enzym. 21 (2003) 113–121.
[5] O. Kagami, K. Shindo, A. Kyojima, K. Takeda, H. Ikenaga, K. Furukawa, N. Misawa, Protein engineering on biphenyl dioxygenase for conferring activity to convert 7-hydroxyflavone and 5,7-dihydroxyflavone (chrysin), J. Biosci. Bioeng. 106 (2008) 121–127.
[6] N. Misawa, R. Nakamura, Y. Kagiyama, H. Ikenaga, K. Furukawa, K. Shindo, Synthesis of vicinal diols from various arenes with a heterocyclic, amino or carboxyl group by using recombinant *Escherichia coli* cells expressing evolved biphenyl dioxygenase and dihydrodiol dehydrogenase genes, Tetrahedron 61 (2005) 195–204.
[7] T.T. Pham, Y. Tu, M. Sylvestre, Remarkable abilities of *Pandoraea pnomenusa* B356 biphenyl dioxygenase to metabolize simple flavonoids, Appl. Environ. Microbiol. 78 (2012) 3560–3570.
[8] J. Seo, S.I. Kang, J.Y. Ryu, Y.J. Lee, K.D. Park, M. Kim, D. Won, H.Y. Park, J.H. Ahn, Y. Chong, R.A. Kanaly, J. Han, H.G. Hur, Location of flavone B-ring controls regioselectivity and stereoselectivity of naphthalene dioxygenase from *Pseudomonas* sp. strain NCIB 9816–4, Appl. Microbiol. Biotechnol. 86 (2010) 1451–1462.
[9] K. Shindo, R. Nakamura, A. Osawa, O. Kagami, K. Kanoh, K. Furukawa, N. Misawa, Biocatalytic synthesis of monocyclic arene-dihydrodiols and -diols by *Escherichia coli* cells expressing hybrid toluene/biphenyl dioxygenase and dihydrodiol dehydrogenase genes, J. Mol. Catal. B: Enzym. 35 (2005) 134–141.
[10] T. Hudlicky, D. Gonzalez, D.T. Gibson, Enzymatic dihydroxylation of aromatics in enantioselective synthesis: Expanding asymmetric methodology, Aldrichimica Acta 32 (1999) 35–62.
[11] J.D. Haddock, D.T. Gibson, Purification and characterization of the oxygenase component of biphenyl 2,3-dioxygenase from *Pseudomonas* sp. strain LB400, J. Bacteriol. 177 (1995) 5834–5839.
[12] Y. Hurtubise, D. Barriault, J. Powlowski, M. Sylvestre, Purification and characterization of the *Comamonas testosteroni* B-356 biphenyl dioxygenase components, J. Bacteriol. 177 (1995) 6610–6618.
[13] Y. Hurtubise, D. Barriault, M. Sylvestre, Characterization of active recombinant his-tagged oxygenase component of *Comamonas testosteroni* B-356 biphenyl dioxygenase, J. Biol. Chem. 271 (1996) 8152–8156.
[14] P. Kumar, M. Mohammadi, J.F. Viger, D. Barriault, L. Gomez-Gil, L.D. Eltis, J.T. Bolin, M. Sylvestre, Structural insight into the expanded PCB-degrading abilities of a biphenyl dioxygenase obtained by directed evolution, J. Mol. Biol. 405 (2011) 531–547.
[15] D. Barriault, M. Sylvestre, Evolution of the biphenyl dioxygenase BphA from *Burkholderia xenovorans* LB400 by random mutagenesis of multiple sites in region III, J. Biol. Chem. 279 (2004) 47480–47488.
[16] J.F. Viger, M. Mohammadi, D. Barriault, M. Sylvestre, Metabolism of chlorobiphenyls by a variant biphenyl dioxygenase exhibiting enhanced activity toward dibenzofuran, Biochem. Biophys. Res. Commun. 419 (2012) 362–367.
[17] S.I. Sato, J.W. Nam, K. Kasuga, H. Nojiri, H. Yamane, T. Omori, Identification and characterization of genes encoding carbazole 1,9a-dioxygenase in *Pseudomonas* sp. strain CA10, J Bacteriol. 179 (1997) 4850–4858.
[18] M. Mohammadi, J.F. Viger, P. Kumar, D. Barriault, J.T. Bolin, M. Sylvestre, Retuning Rieske-type oxygenases to expand substrate range, J. Biol. Chem. 286 (2011) 27612–27621.
[19] P. Kumar, L. Gomez-Gil, M. Mohammadi, M. Sylvestre, L.D. Eltis, J.T. Bolin, Anaerobic crystallization and initial X-ray diffraction data of biphenyl 2,3-dioxygenase from *Burkholderia xenovorans* LB400: Addition of agarose improved the quality of the crystals, Acta Crystallogr., Sect. F: Struct. Biol. Cryst. Commun. 67 (2011) 59–62.
[20] Z. Otwinowski, W. Minor, Processing of X-ray diffraction data collected in oscillation mode, Methods Enzymol. 276 (1997) 307–326.
[21] A. Vagin, A. Teplyakov, MOLREP: An automated program for molecular replacement, J. Appl. Crystallogr. 30 (1997) 1022–1025.
[22] Collaborative, Computational, and Project, The CCP4 suite: programs for protein crystallography, Acta Crystallogr.,Sec. D: Biol. Crystallogr. 50 (1994) 760–3.
[23] A.T. Brünger, P.D. Adams, G.M. Clore, W.L. DeLano, P. Gros, R.W. Grosse-Kunstleve, J.S. Jiang, J. Kuszewski, M. Nilges, N.S. Pannu, R.J. Read, L.M. Rice, T. Simonson, G.L. Warren, Crystallography & NMR system: A new software suite for macromolecular structure determination, Acta Crystallogr.,Sec. D: Biol. Crystallogr. 54 (1998) 905–921.
[24] G.N. Murshudov, A.A. Vagin, E.J. Dodson, Refinement of macromolecular structures by the maximum-likelihood method, Acta Crystallogr.,Sec. D: Biol. Crystallogr. 53 (1997) 240–255.
[25] Y. Ashikawa, Z. Fujimoto, H. Noguchi, H. Habe, T. Omori, H. Yamane, H. Nojiri, Electron transfer complex formation between oxygenase and ferredoxin components in Rieske nonheme iron oxygenase system, Structure 14 (2006) 1779–1789.
[26] J. Dundas, Z. Ouyang, J. Tseng, A. Binkowski, Y. Turpaz, J. Liang, CASTp: Computed atlas of surface topography of proteins with structural and topographical mapping of functionally annotated residues, Nucleic Acids Res. 34 (2006) W116–W118.
[27] W.L. DeLano, The PyMOL Molecular Graphics System, Schrödinger, LLC, New York, 2002.
[28] A. Karlsson, J.V. Parales, R.E. Parales, D.T. Gibson, H. Eklund, S. Ramaswamy, Crystal structure of naphthalene dioxygenase: Side-on binding of dioxygen to iron, Science 299 (2003) 1039–1042.
[29] H. Nojiri, Y. Ashikawa, H. Noguchi, J.W. Nam, M. Urata, Z. Fujimoto, H. Uchimura, T. Terada, S. Nakamura, K. Shimizu, T. Yoshida, H. Habe, T. Omori, Structure of the terminal oxygenase component of angular dioxygenase, carbazole 1,9a-dioxygenase, J. Mol. Biol. 351 (2005) 355–370.
[30] D.J. Ferraro, L. Gakhar, S. Ramaswamy, Rieske business: Structure-function of Rieske non-heme oxygenases, Biochem. Biophys. Res. Commun. 338 (2005) 175–190.
[31] R.E. Parales, J.V. Parales, D.T. Gibson, Aspartate 205 in the catalytic domain of naphthalene dioxygenase is essential for activity, J. Bacteriol. 181 (1999) 1831–1837.
[32] K. Inoue, Y. Ashikawa, T. Umeda, M. Abo, J. Katsuki, Y. Usami, H. Noguchi, Z. Fujimoto, T. Terada, H. Yamane, H. Nojiri, Specific interactions between the ferredoxin and terminal oxygenase components of a class IIB Rieske nonheme iron oxygenase, carbazole 1,9a-dioxygenase, J. Mol. Biol. 392 (2009) 436–451.
[33] B.M. Martins, T. Svetlitchnaia, H. Dobbek, 2-Oxoquinoline 8-monooxygenase oxygenase component: Active site modulation by Rieske-[2Fe-2S] center oxidation/reduction, Structure 13 (2005) 817–824.